Semiclassical Models for the Schrödinger Equation with Periodic Potentials and Band Crossings*

Lihui Chai[†] Shi Jin[‡] Qin Li[§]

Contents

Abstract

The Bloch decomposition plays a fundamental role in the study of quantum mechanics and wave propagation in periodic media. Most of the homogenization theory developed for the study of high frequency or semiclassical limit for these problems assumes no crossing of the Bloch bands, resulting in classical Liouville equations in the limit along each Bloch band.

In this article, we derive semiclassical models for the Schrödinger equation in periodic media that take into account band crossing, which is important to describe quantum transitions between Bloch bands. Our idea is still based on the Wigner transform (on the Bloch eigenfunctions), but in taking the semiclassical approximation, we retain the off-diagonal entries of the Wigner matrix, which cannot be ignored near the point of band crossing. This results in coupled inhomogenious Liouville systems that can suitably describe quantum tunnelling between bands that are not well-separated. We also develop a domain decomposition method that couples these semiclassical models with the classical Liouville equations (valid away from zones of band crossing) for a multiscale computation. Solutions of these models are numerically compared with those of the Schröding equation to justify the validity of these new models for band-crossings.

1 Introduction

The linear Schrödinger equation with a periodic potential is an important model in solid state physics. It describes the motion of electrons in a crystal with a lattice structure. We consider the following one dimensional Schrödinger equation

$$i\varepsilon\phi_t^\varepsilon = -\frac{\varepsilon^2}{2}\phi_{xx}^\varepsilon + \left(V\left(\frac{x}{\varepsilon}\right) + U(x)\right)\phi^\varepsilon, \quad t > 0, \quad x \in \mathbb{R}. \tag{1.1}$$

Here, ϕ^ε is the complex-valued wave function, ε is the dimensionless rescaled Planck constant, $V(x)$ is a periodic potential with the lattice $L = 2\pi\mathbb{Z}$, so $V(x + \nu) = V(x)$ for any $x \in \mathbb{R}$ and $\nu \in L$. $U(x)$ is a smooth external potential function. We denote the dual lattice of L by L^* and $L^* = \mathbb{Z}$. The fundamental domain of L is $(0, 2\pi)$ and the first Brillouin zone is $\mathcal{B} = \left(-\frac{1}{2}, \frac{1}{2}\right)$.

In the semi-classical regime $\varepsilon \ll 1$, the Schrödinger equation has a semi-classical limit governed by the Liouville system [31], which was justified rigorously in [10, 21, 22]. It has been shown that the electrons remain in a certain quantum subsystem, "move along the m-th band" and the dynamics is given by $\dot{x} = \partial_k E_m(k)$, where E_m is the energy corresponding to the m-th *Bloch band* [2]. Higher order correction relevant to Berry phase can be included, see [24, 25, 8]. All of these results use the *adiabatic* assumption, namely, different Bloch bands are well-separated and there is no band-crossing.

The *non-adiabatic* or *diabatic* effect should be considered whenever the transitions between energy levels of the quantum system play an important role. This may happen when the gap between the energy levels becomes small enough in comparison to the scaled Planck constant ε. The well-known Landau-Zener formula [18, 32] describes the asymptotic effect of avoided crossings in various specific situations. The study of such "qunatum tunnellings" is important in many applications, from quantum dynamics in chemical reaction [30], semiconductors to Bose-Einstein condensation [3]. While in the case of band separation there have been significant mathematical progress in understanding the semiclassical limit [1, 10, 22, 24, 25], as well as numerical methods that utilizes the Bloch decomposition [14], there has been little mathematical and computational works for the band-mixing case. In the context of "surface hopping method", associated with the Born-Oppenheimer approximation, the Landau-Zener phenomenon has been studied computationally by Tully etc. [30, 29, 26, 7] and mathematically [12, 9, 20, 19]. For a Liouville equation based computational approach, see [16], and a quantum-classical model for surface hopping, see [23, 13].

In this paper, we use the Wigner-Bloch theory to derive semiclassical models for the Schrödinger equation with periodic potentials (1.1) that account for band-crossing. Without band-crossing, the classical Liouville equation can be obtained along each Bloch band [1, 10, 22], as $\varepsilon \to 0$. This only includes the diagonal entries of the Wigner-Bloch matrix (the Wigner transform of the Bloch functions) which is valid away from the crossing zone. In our semiclassical models we include the leading order of the off-diagonal entries, resulting in system of complex, inhomogeneous Liouville equations. These systems contain terms that describe for transitions between bands, as well as Berry phase information which is related to the quantum Hall effect [28]. These systems are still hyperbolic, with oscillatory forcing terms that converge (in the weak sense) to zero in the semiclassical limit away from band-crossing zones so the classical Liouville equation can be recovered. Several numerical experiments using these models produce numerical solutions that adequately describe the quantum transitions between bands, when compared with the solutions of the original Schrödinger equation (1.1).

The computational cost of these semiclassical models, while considerably lower than that of the original Schröginer equation, is higher than the adiabatic Liouville equations without band-crossing. In order to further reduce the computational cost, a hybrid method that couples the classical Liouville equation away from the crossing zone to the new semiclassical models to be used in the crossing zones is introduced. A couple of other more efficient computational approaches for linear periodic potentials, are also introduced in section 5.

This paper is organized as follows. In Section 2, we introduce the Wigner transform and the Bloch eigenvalue problem that are the two tools to study the semiclassical limit of the Schrödinger equation with periodic potentials. We also review the classical limit without band-crossing which gives rise to the classical Liouville equation for each Bloch band. In Section 3 we derive the new semi-classical Liouville systems that account for quantum transitions between different bands. In Section 4 we introduce a domain-decomposition based hybrid model that couples the classical Liouville systme away from the band crossing zone to the new semiclassical models used in the crossing zones. Some numerical examples are presented in Section 5 to validate these semiclassical models for quantum transions between Bloch bands. More efficient numerical methods were introduced for simpler linear potentials. Section 6 concludes this paper.

2 The classical limit without band-crossing

2.1 The Wigner transform

Define the asymmetric Wigner transformation as in [1],

$$W_\varepsilon(t,x,k) = \int_\mathbb{R} \frac{\mathrm{d}y}{2\pi} \mathrm{e}^{\mathrm{i}ky} \phi^\varepsilon(t, x-\varepsilon y) \, \bar{\phi}^\varepsilon(t,x). \tag{2.1}$$

where $\bar{\phi}^\varepsilon$ is the complex conjugate of ϕ^ε, and ϕ^ε is the solution to the Schrödinger equation (1.1), then one obtains the Wigner equation:

$$\frac{\partial W_\varepsilon}{\partial t} + k\frac{\partial W_\varepsilon}{\partial x} + \frac{\mathrm{i}\varepsilon}{2}\frac{\partial^2 W_\varepsilon}{\partial x^2} = \frac{1}{\mathrm{i}\varepsilon} \sum_{\mu \in L^*} \mathrm{e}^{\mathrm{i}\mu x/\varepsilon} \hat{V}(\mu) \left[W_\varepsilon(x, k-\mu) - W_\varepsilon(x,k) \right] \tag{2.2}$$

$$+ \frac{1}{\mathrm{i}\varepsilon} \int_\mathbb{R} \frac{\mathrm{d}\omega}{2\pi} \mathrm{e}^{\mathrm{i}\omega x} \hat{U}(\omega) \left[W_\varepsilon(x, k-\varepsilon\omega) - W_\varepsilon(x,k) \right],$$

where $\hat{U}(\omega)$ is the Fourier transform of $U(y)$:

$$\hat{U}(\omega) = \int_\mathbb{R} \mathrm{d}y \, \mathrm{e}^{-\mathrm{i}\omega y} U(y), \quad \omega \in \mathbb{R}, \tag{2.3}$$

and $\hat{V}(\mu)$ is the discrete Fourier coefficients of $V(y)$:

$$\hat{V}(\mu) = \frac{1}{2\pi} \int_0^{2\pi} \mathrm{d}y \, \mathrm{e}^{-\mathrm{i}\mu y} V(y), \quad \mu \in L^*. \tag{2.4}$$

Here $(0, 2\pi)$ is the fundamental domain of the lattice L.

Denote $z = \frac{x}{\varepsilon}$ as the fast variable. To separate the dependence on both the slow and the fast variables, one can write $W_\varepsilon(t,x,k)$ as $W_\varepsilon(t,x,z,k)$, and replace the spatial derivative $\frac{\partial}{\partial x}$ by $\frac{\partial}{\partial x} + \frac{1}{\varepsilon}\frac{\partial}{\partial z}$. Then (2.2) becomes:

$$\frac{\partial}{\partial t}W_\varepsilon + k\left(\frac{\partial}{\partial x} + \frac{1}{\varepsilon}\frac{\partial}{\partial z}\right)W_\varepsilon + \frac{\mathrm{i}\varepsilon}{2}\left(\frac{\partial}{\partial x} + \frac{1}{\varepsilon}\frac{\partial}{\partial z}\right)^2 W_\varepsilon$$

$$= \frac{1}{\mathrm{i}\varepsilon} \sum_{\mu \in L^*} \mathrm{e}^{\mathrm{i}\mu x/\varepsilon} \hat{V}(\mu) \left[W_\varepsilon(x, k-\mu) - W_\varepsilon(x,k) \right] \tag{2.5}$$

$$+ \frac{1}{\mathrm{i}\varepsilon} \int_\mathbb{R} \frac{\mathrm{d}\omega}{2\pi} \mathrm{e}^{\mathrm{i}\omega x} \hat{U}(\omega) \left[W_\varepsilon(x, k-\varepsilon\omega) - W_\varepsilon(x,k) \right].$$

Assume $U(x)$ is smooth enough, one throws away high order terms, and (2.5) becomes:

$$\frac{\partial W_\varepsilon}{\partial t} + k\frac{\partial W_\varepsilon}{\partial x} - \frac{\partial U}{\partial x}\frac{\partial W_\varepsilon}{\partial k} + \mathrm{i}\frac{\partial^2 W_\varepsilon}{\partial x \partial z} = -\frac{1}{\varepsilon}\mathcal{L}W_\varepsilon, \tag{2.6}$$

where the skew symmetric operator $\mathcal{L}$ is given by

$$\mathcal{L}f(z,k) = k\frac{\partial f}{\partial z} + \frac{\mathrm{i}}{2}\frac{\partial^2 f}{\partial z^2} - \frac{1}{\mathrm{i}} \sum_{\mu \in L^*} \mathrm{e}^{\mathrm{i}\mu x/\varepsilon} \hat{V}(\mu) \left[f(x, k-\mu) - f(x,k) \right].$$

Asymptotically one expands W_ε by:

$$W_\varepsilon(t, x, k) = W_0\left(t, x, \frac{x}{\varepsilon}, k\right) + \varepsilon W_1\left(t, x, \frac{x}{\varepsilon}, k\right) + \cdots \tag{2.7}$$

and plugs this ansatz into (2.5). In the order of $\mathcal{O}(\frac{1}{\varepsilon})$ and $\mathcal{O}(1)$ respectively, one gets:

$$\mathcal{L}W_0 = 0, \tag{2.8a}$$

$$\frac{\partial W_0}{\partial t} + k\frac{\partial W_0}{\partial x} - \frac{\partial U}{\partial x}\frac{\partial W_0}{\partial k} + i\frac{\partial^2 W_0}{\partial x \partial z} = -\mathcal{L}W_1. \tag{2.8b}$$

This implies that W_0 is in the kernel of $\mathcal{L}$. We seek a good basis of $\ker\mathcal{L}$ in section 2.2, and leave the exact formulation of W_0 to section 2.3.

2.2   The Bloch eigenvalue problem

The eigenfunctions of $\mathcal{L}$ are constructed by studying the following eigenvalue problem:

$$-\frac{1}{2}\frac{\partial^2}{\partial z^2}\Psi(z, p) + V(z)\Psi(z, p) = E(p)\Psi(z, p), \tag{2.9a}$$

$$\Psi(z + \nu, p) = e^{ip\nu}\Psi(z, p), \quad \forall \nu \in L, \tag{2.9b}$$

$$\frac{\partial\Psi}{\partial z}(z + \nu, p) = e^{ip\nu}\frac{\partial\Psi}{\partial z}(z, p), \quad \forall \nu \in L. \tag{2.9c}$$

With each specific p, one constructs a boundary condition (2.9b,2.9c) and solves the eigenvalue problem. Denote $E_m(p)$ as the m-th eigenvalue with multiplicity r_m, and Ψ_m^α, with $\alpha = 1, ..., r_m$, as the associated α-th eigenfunction. Ψ_m is usually called the m-th Bloch eigenfunction [2]. For this problem, one can easily check the following properties:

(a) The eigenvalues $E_m(p)$ are L^*-periodic in p and have constant finite multiplicity outside a closed zero-measure subset F of $p \in \mathbb{R}$. Outside F, one orders the eigenvalues as $E_1(p) < E_2(p) < ... < E_m(p) < ...$ with $E_m(p) \to \infty$ as $m \to \infty$, uniformly in p.

(b) For any $p \in \left(-\frac{1}{2}, \frac{1}{2}\right)$, $\{\Psi_m^\alpha(\cdot, p)\}$ forms a complete orthonormal basis in $L^2(0, 2\pi)$, i.e.

$$(\Psi_m^\alpha, \Psi_n^\beta) := \int_0^{2\pi} \frac{\mathrm{d}z}{2\pi}\Psi_m^\alpha(z, p)\bar{\Psi}_n^\beta(z, p) = \delta_{mn}\delta_{\alpha\beta}. \tag{2.10}$$

(c) For all $\phi \in L^2(\mathbb{R})$, one has the following Bloch decomposition:

$$\phi(x) = \sum_m^\infty \sum_{\alpha=1}^{r_m} \int_{\mathcal{B}} c_m^\alpha(p)\Psi_m^\alpha(x, p)\,\mathrm{d}p \tag{2.11}$$

where c_m^α is the Bloch coefficient: $c_m^\alpha(p) = \int_{\mathbb{R}} \phi(x)\bar{\Psi}_m^\alpha(x, p)\,\mathrm{d}x$.

Define

$$\Phi_m^\alpha(z,p) = \mathrm{e}^{-\mathrm{i}pz}\,\Psi_m^\alpha(z,p), \tag{2.12}$$

then Φ_m^α is a $z-$periodic function with period 2π. For any $p \in \left(-\frac{1}{2}, \frac{1}{2}\right)$, $\{\Phi_m^\alpha(\cdot, p)\}$ forms a complete orthonormal basis in $L^2(0, 2\pi)$.

For simplicity, throughout this paper we make the following assumption:

Assumption 1. The multiplicity for each eigenvalue E_m is 1 outside F. We will drop the superscript α when there is no ambiguity.

2.3 The classical limit without band-crossing

In this section, we review the classical limit without band-crossing [1]. For that, we need the following assumption:

Assumption 2. The set F is a null set, i.e. eigenvalues are strictly apart from each other everywhere in p, namely $E_1(p) < E_2(p) < ... < E_j(p) < ...$.

By taking the Wigner transformation on the Bloch eigenfunctions, one obtains a basis on the phase space. Define the $z-$periodic functions $Q_{mn}(z, k)$ by:

$$Q_{mn}(z,k) = Q_{mn}(z, \mu_k, p_k) = \int_0^{2\pi} \frac{\mathrm{d}y}{2\pi} \mathrm{e}^{\mathrm{i}ky} \Psi_m(z - y, p_k)\bar{\Psi}_n(z, p_k), \tag{2.13}$$

where k is an arbitrary real number and is decomposed as:

$$k = p_k + \mu_k, \quad p_k \in \mathcal{B}, \ \mu_k \in L^*. \tag{2.14}$$

Lemma 2.1. Define the inner product $\langle \cdot, \cdot \rangle$:

$$\langle f, g \rangle := \sum_{\mu \in L^*} \int_0^{2\pi} \frac{\mathrm{d}z}{2\pi} f(z, \mu)\bar{g}(z, \mu), \quad f, g \in L^2\big((0, 2\pi), \ell^2(L^*)\big),$$

then for any $p \in (-1/2, 1/2)$, $\{Q_{mn}(\cdot, \cdot, p)\}$ forms a complete orthonormal basis in $L^2\big((0, 2\pi) \times \ell^2(L^*)\big)$.

Proof. The orthonormal condition

$$\langle Q_{mn}, Q_{jl} \rangle = \delta_{mj}\,\delta_{nl}, \tag{2.15}$$

can be proved by simply using (2.10). To prove the completeness, it is sufficient to show that: if there exists an $f \in L^2\big((0, 2\pi) \times \ell^2(L^*)\big)$, such that $\langle f, Q_{mn} \rangle = 0$ for all $m, n \in \mathbb{N}$, then $f(z, \mu) \equiv 0$. Assume $\langle f, Q_{mn} \rangle = 0$ for all $m, n \in \mathbb{N}$. By the definition of Q_{mn},

$$\sum_\mu \int_0^{2\pi} \int_0^{2\pi} \frac{\mathrm{d}y\mathrm{d}z}{(2\pi)^2} f(z, \mu)\mathrm{e}^{\mathrm{i}\mu y}\Phi_m(z - y, p)\bar{\Phi}_n(z, p) = 0, \quad \forall m, n \in \mathbb{N}.$$

Since $\{\Phi_n(\cdot, p)\}$ forms a complete orthonormal basis in $L^2(0, 2\pi)$, the above equality implies that

$$\sum_\mu \int_0^{2\pi} \frac{\mathrm{d}y}{2\pi} f(z, \mu) \mathrm{e}^{\mathrm{i}\mu y} \Phi_m(z - y, p) = 0, \quad \forall m \in \mathbb{N},$$

thus

$$\sum_\mu f(z, \mu) \mathrm{e}^{\mathrm{i}\mu y} \equiv 0,$$

which implies that $f(z, \mu) \equiv 0$. $\qquad\qquad\qquad\qquad\qquad\qquad\qquad\qquad\qquad$ $\square$

A straightforward computation gives:

$$\mathcal{L}Q_{mn}(z, k) = \mathcal{L}Q_{mn}(z, \mu, p) = \mathrm{i}(E_m(p) - E_n(p))Q_{mn}(z, \mu, p). \tag{2.16}$$

Apparently, under Assumptions 1 and 2, (2.16) gives:

$$\ker\mathcal{L} = \mathrm{span}\{Q_{mm}, m = 1, 2, \cdots\}. \tag{2.17}$$

Therefore, from (2.8a) W_0 has the form

$$W_0(t, x, z, k) = \sum_m \sigma_{mm}(t, x, p)Q_{mm}(z, \mu, p), \tag{2.18}$$

with σ_{mm} representing the expansion coefficients. To derive the equation for them, one plugs it back into (2.8b), and takes the inner product with Q_{mm} on both sides, the right hand side vanishes due to the skew symmetry of $\mathcal{L}$ and (2.16):

$$\langle -\mathcal{L}W_1, Q_{mm} \rangle = \langle -W_1, \mathcal{L}Q_{mm} \rangle = 0. \tag{2.19}$$

The left hand side, on the other hand, gives:

$$\langle \partial_t W_0 + k\partial_x W_0 - \partial_x U \partial_k W_0 + \mathrm{i}\partial_{xz} W_0, Q_{mm} \rangle$$
$$= \sum_n \partial_t \sigma_{nn} \langle Q_{nn}, Q_{mm} \rangle + \sum_{nn} \partial_x \sigma_{nn} \langle kQ_{nn}, Q_{mm} \rangle$$
$$\quad - \partial_x U \left(\sum_n \partial_p \sigma_{nn} \langle Q_{nn}, Q_{mm} \rangle + \sum_{nn} \sigma_m \langle \partial_p Q_{nn}, Q_{mm} \rangle \right)$$
$$= \partial_t \sigma_{mm} + \partial_p E_m \partial_x \sigma_{mm} - \partial_x U \partial_p \sigma_{mm}. \tag{2.20}$$

Thus one can combine (2.19) and (2.20), and obtain:

$$\partial_t \sigma_{mm} + \partial_p E_m \partial_x \sigma_{mm} - \partial_x U \partial_p \sigma_{mm} = 0. \tag{2.21}$$

8

In the derivation of (2.20), the following equalities were used :

$$\langle kQ_{mn}, Q_{jl} \rangle = -\frac{\mathrm{i}}{2} \big(\delta_{nl} \left(\partial_z \Psi_m, \Psi_j \right) + \delta_{mj} \left(\partial_z \Psi_l, \Psi_n \right) \big), \tag{2.22a}$$

$$\langle \partial_p Q_{mn}, Q_{jl} \rangle = \delta_{nl} \left(\partial_p \Phi_m, \Phi_j \right) + \delta_{mj} \left(\Phi_l, \partial_p \Phi_n \right), \tag{2.22b}$$

$$\langle \partial_z Q_{mn}, Q_{jl} \rangle = \delta_{nl} \left(\partial_z \Psi_m, \Psi_j \right) - \delta_{mj} \left(\partial_z \Psi_l, \Psi_n \right), \tag{2.22c}$$

$$\partial_p E_m \delta_{mj} + \left(\partial_p \Phi_m, \, \Phi_j \right) \left(E_m - E_j \right) = -\mathrm{i} \left(\partial_z \Psi_m, \, \Psi_j \right), \tag{2.22d}$$

$$\left(\partial_p \Phi_m, \Phi_m \right) + \left(\Phi_m, \partial_p \Phi_m \right) = 0. \tag{2.22e}$$

The details can also be found in [1].

Notice that 2.21 is the classical Liouville equation for each Bloch band.

Remark 2.1. Similar results were rigorously proved in [22, 10].

3   Asymptotic models for the band-to-band transition

This section is for the case when Assumption 2 is not satisfied. Physically, ε is small but nonzero, and electrons can tunnel across bands for all p. But this tunneling is negligible when bands are far away from each other, the so-called *adiabatic* assumption. This is the basis for the asymptotically expansion (2.18), which throws away the dependence on the band-transition terms $Q_{mn}(m \neq n)$ of W_0. However, if there exists $m_0 \neq n_0$ and a point p_c, such that $|E_{m_0}(p_c) - E_{n_0}(p_c)| \sim O(\varepsilon)$, then $\mathcal{L}Q_{m_0 n_0} \sim O(\varepsilon)$, so the asymptotic expansion (2.8) does not hold any more. When this happens, physically one observes significant tunneling effect. We seek asymptotic models to handle the band-to-band transition in this section.

3.1   The derivation of a two-band semi-classical Liouville system using the asymmetric Wigner transform

In order to handle the band-to-band transition phenomena, we come back to the asymptotic model (2.6) and use the following expression (compare with (2.18)!):

$$W_\varepsilon = \sum_m \sigma_{mm} Q_{mm} + \sum_{m \neq n} \sigma_{mn} Q_{mn}. \tag{3.1}$$

Without loss of generality, we tackle a two-band problem. Define $p_c = \arg\min_p \{|E_1 - E_2|\}$ and assume $|E_1(p_c) - E_2(p_c)| = \mathcal{O}(\varepsilon)$ and $p_c = 0$.

Plugging (3.1) into (2.6) and taking the inner product with Q_{mn} as mentioned in Sec. 2.3, one gets a system for σ_{mn}'s:

$$\frac{\partial \sigma_{11}}{\partial t} + \frac{\partial E_1}{\partial p}\frac{\partial \sigma_{11}}{\partial x} + \frac{1}{i}\left(\frac{\partial \Psi_1}{\partial z}, \Psi_2\right)\frac{\partial \sigma_{12}}{\partial x} - \frac{\partial U}{\partial x}\frac{\partial \sigma_{11}}{\partial p}$$
$$= \frac{\partial U}{\partial x}\left[\left(\frac{\partial \Phi_2}{\partial p}, \Phi_1\right)\sigma_{21} + \left(\Phi_1, \frac{\partial \Phi_2}{\partial p}\right)\sigma_{12}\right],$$

$$\frac{\partial \sigma_{22}}{\partial t} + \frac{\partial E_2}{\partial p}\frac{\partial \sigma_{22}}{\partial x} + \frac{1}{i}\left(\frac{\partial \Psi_2}{\partial z}, \Psi_1\right)\frac{\partial \sigma_{21}}{\partial x} - \frac{\partial U}{\partial x}\frac{\partial \sigma_{22}}{\partial p}$$
$$= \frac{\partial U}{\partial x}\left[\left(\frac{\partial \Phi_1}{\partial p}, \Phi_2\right)\sigma_{12} + \left(\Phi_2, \frac{\partial \Phi_1}{\partial p}\right)\sigma_{21}\right],$$

$$\frac{\partial \sigma_{12}}{\partial t} + \frac{\partial E_2}{\partial p}\frac{\partial \sigma_{12}}{\partial x} + \frac{1}{i}\left(\frac{\partial \Psi_2}{\partial z}, \Psi_1\right)\frac{\partial \sigma_{11}}{\partial x} - \frac{\partial U}{\partial x}\frac{\partial \sigma_{12}}{\partial p} + i\frac{E_1 - E_2}{\varepsilon}\sigma_{12}$$
$$= \frac{\partial U}{\partial x}\left[\left(\Phi_2, \frac{\partial \Phi_1}{\partial p}\right)\sigma_{11} + \left(\frac{\partial \Phi_2}{\partial p}, \Phi_1\right)\sigma_{22} + \left(\Phi_2, \frac{\partial \Phi_2}{\partial p}\right)\sigma_{12} + \left(\frac{\partial \Phi_1}{\partial p}, \Phi_1\right)\sigma_{12}\right],$$

$$\frac{\partial \sigma_{21}}{\partial t} + \frac{\partial E_1}{\partial p}\frac{\partial \sigma_{21}}{\partial x} + \frac{1}{i}\left(\frac{\partial \Psi_1}{\partial z}, \Psi_2\right)\frac{\partial \sigma_{22}}{\partial x} - \frac{\partial U}{\partial x}\frac{\partial \sigma_{21}}{\partial p} + i\frac{E_2 - E_1}{\varepsilon}\sigma_{21}$$
$$= \frac{\partial U}{\partial x}\left[\left(\Phi_1, \frac{\partial \Phi_2}{\partial p}\right)\sigma_{22} + \left(\frac{\partial \Phi_1}{\partial p}, \Phi_2\right)\sigma_{11} + \left(\Phi_1, \frac{\partial \Phi_1}{\partial p}\right)\sigma_{21} + \left(\frac{\partial \Phi_2}{\partial p}, \Phi_2\right)\sigma_{21}\right].$$

This system can be written in vector form as:

$$\partial_t \boldsymbol{\sigma} + A\partial_x \boldsymbol{\sigma} + B\partial_p \boldsymbol{\sigma} = -BC\boldsymbol{\sigma} + \frac{iD}{\varepsilon}\boldsymbol{\sigma} \tag{3.2a}$$

where

$$\boldsymbol{\sigma} = \begin{pmatrix} \sigma_{11} & \sigma_{12} & \sigma_{21} & \sigma_{22} \end{pmatrix}^T \tag{3.2b}$$

$$B = -\partial_x U\, \mathbb{I}, \quad D = \text{diag}\begin{pmatrix} 0, E_2 - E_1, E_1 - E_2, 0 \end{pmatrix} \tag{3.2c}$$

$$A = \begin{bmatrix} \partial_p E_1 & \psi_{12} & 0 & 0 \\ \psi_{21} & \partial_p E_2 & 0 & 0 \\ 0 & 0 & \partial_p E_1 & \psi_{12} \\ 0 & 0 & \psi_{21} & \partial_p E_2 \end{bmatrix}, \tag{3.2d}$$

$$C = \begin{bmatrix} 0 & -\phi_{12} & \phi_{21} & 0 \\ -\phi_{21} & \phi_{11} - \phi_{22} & 0 & \phi_{21} \\ \phi_{12} & 0 & \phi_{22} - \phi_{11} & -\phi_{12} \\ 0 & \phi_{12} & -\phi_{21} & 0 \end{bmatrix}, \tag{3.2e}$$

$$\psi_{mn} = -i\left(\partial_z \Psi_m, \Psi_n\right), \text{ and } \phi_{mn} = \left(\partial_p \Phi_m, \Phi_n\right), \tag{3.2f}$$

Where the superscript T denotes the matrix transpose, $\mathbb{I}$ is the identity matrix. Generally, $\psi_{12} = \bar{\psi}_{21}$, $\phi_{12} = -\bar{\phi}_{21}$ are complex-valued quantities, and ϕ_{11}, ϕ_{22} are purely imaginary, so $A = A^\dagger$ is Hermitian, and $C = -C^\dagger$ is anti-Hermitian (where the superscript $\dagger$ denotes the matrix conjugate transpose). Note that $\partial_x U \phi_{mm}$ is the so-called Berry-phase [4, 25, 28].

It can be shown the system (3.2) is a *hyperbolic* system (see the details in Appendix A). Since the source matrix $C = -C^\dagger$, all of its eigenvalues are purely imaginary. Thus this system has unique bounded solution if the initial data are bounded [6] uniformly in *varepsilon*.

For later convenience, we call the semi-classical Liouville system (3.2) Liouville-A system, and this is the system that will be discussed and numerically solved in the paper.

One also needs to equip it with appropriate initial condition. Choose the initial data of the Schrödinger equation as two wave packets along the two Bloch bands in the following form [4, 14]:

$$\phi_I = a_1(x)\,\Phi_1\left(\frac{x}{\varepsilon}, \partial_x S_0(x)\right)\, \mathrm{e}^{\mathrm{i}S_0(x)/\varepsilon} + a_2(x)\,\Phi_2\left(\frac{x}{\varepsilon}, \partial_x S_0(x)\right)\, \mathrm{e}^{\mathrm{i}S_0(x)/\varepsilon}. \tag{3.3}$$

Then, the initial data of the Wigner function, for $\varepsilon \ll 1$, has the approximation:

$$\begin{aligned} W_I(x, z, k) &\sim |a_1(x)|^2 W_{11}(z, k) + |a_2(x)|^2 W_{22}(z, k) \\ &\quad + a_1(x)a_2(x)\big(W_{12}(z, k) + W_{21}(z, k)\big), \end{aligned} \tag{3.4}$$

with

$$W_{mn}(z, k) = \int_{\mathbb{R}} \frac{\mathrm{d}y}{2\pi} \mathrm{e}^{\mathrm{i}ky} \Phi_m(z - y, \partial_x S_0(x - \varepsilon y)) \bar{\Phi}_n(z, \partial_x S_0(x)) \mathrm{e}^{\mathrm{i}(S_0(x - \varepsilon y) - S_0(x))/\varepsilon}.$$

Using Taylor expansion on $S_0(x - \varepsilon y) - S_0(x)$ and $\Phi_m(z - y, \partial_x S_0(x - \varepsilon y))$, one gets

$$W_{mn}(z, k) = \int_{\mathbb{R}} \frac{\mathrm{d}y}{2\pi} \mathrm{e}^{\mathrm{i}(k - \partial_x S_0(x))y} \Phi_m(z - y, \partial_x S_0(x)) \bar{\Phi}_n(z, \partial_x S_0(x)) + \mathcal{O}(\varepsilon),$$

then by ignoring the $\mathcal{O}(\varepsilon)$ term, and using the periodicity of $\Phi_m(z, p)$ on z, one can change the integral into a summation of integrals from 0 to 2π:

$$W_{mn}(z, k) = \sum_{\nu \in L} \int_0^{2\pi} \frac{\mathrm{d}y}{2\pi} \mathrm{e}^{\mathrm{i}(k - \partial_x S_0(x))(y + \nu)} \Phi_m(z - y, \partial_x S_0(x)) \bar{\Phi}_n(z, \partial_x S_0(x)).$$

Applying the equality

$$\sum_{\nu \in L} \mathrm{e}^{\mathrm{i}k\nu} = \sum_{\mu \in L^*} \delta(k + \mu),$$

11

one gets

$$
\begin{aligned}
W_{mn}(z,k) &= \sum_{\mu \in L^*} \delta(k + \mu - \partial_x S_0) \int_0^{2\pi} \frac{\mathrm{d}y}{2\pi} \mathrm{e}^{\mathrm{i}(k - \partial_x S_0)y} \Phi_m(z - y, \partial_x S_0) \bar{\Phi}_n(z, \partial_x S_0) \\
&= \sum_{\mu \in L^*} \delta(p_k + \mu - \partial_x S_0) \int_0^{2\pi} \frac{\mathrm{d}y}{2\pi} \mathrm{e}^{\mathrm{i}ky} \Psi_m(z - y, \partial_x S_0) \bar{\Psi}_n(z, \partial_x S_0) \\
&= \sum_{\mu \in L^*} \delta(p_k + \mu - \partial_x S_0) \int_0^{2\pi} \frac{\mathrm{d}y}{2\pi} \mathrm{e}^{\mathrm{i}ky} \Psi_m(z - y, p_k + \mu) \bar{\Psi}_n(z, p_k + \mu) \\
&= \sum_{\mu \in L^*} \delta(p_k + \mu - \partial_x S_0) \int_0^{2\pi} \frac{\mathrm{d}y}{2\pi} \mathrm{e}^{\mathrm{i}ky} \Psi_m(z - y, p_k) \bar{\Psi}_n(z, p_k) \\
&= \sum_{\mu \in L^*} \delta\big(p_k + \mu - \partial_x S_0\big) Q_{mn}(z, \mu_k, p_k). \quad (3.5)
\end{aligned}
$$

In the above derivation, from the second line to the third line, we use the fact that

$$
\int \delta(p - p_0) f(p_0) g(p) \, \mathrm{d}p = f(p_0) g(p_0) = \int \delta(p - p_0) f(p) g(p) \, \mathrm{d}p
$$

to replace the argument $\partial_x S_0$ to $p_k + \mu$.

Without loss of generality, we assume that $\partial_x S_0 \in (-1/2, \, 1/2)$, then (3.5) becomes

$$
W_{mn}(z,k) = \delta\big(p_k - \partial_x S_0\big) Q_{mn}(z, \mu_k, p_k). \quad (3.6)
$$

Compare (3.6) with (3.4), one has the initial data for $\boldsymbol{\sigma}$:

$$
\boldsymbol{\sigma}(0, x, p) = \delta\left(p - \partial_x S_0(x)\right) \begin{pmatrix} a_1^2 & a_1 a_2 & a_1 a_2 & a_2^2 \end{pmatrix}^T. \quad (3.7)
$$

3.2 The semi-classical Liouville system using the symmetric Wigner transform

All the analysis above is done in the framework of the asymmetric Wigner transform (2.1). One could also use the symmetric Wigner transform:

$$
W_\varepsilon^s(t, x, k) = \int_\mathbb{R} \frac{\mathrm{d}y}{2\pi} \mathrm{e}^{\mathrm{i}ky} \phi^\varepsilon\left(t, x - \frac{\varepsilon y}{2}\right) \bar{\phi}^\varepsilon\left(t, x + \frac{\varepsilon y}{2}\right). \quad (3.8)
$$

The derivation is similar, thus we skip the details, and give a list of the results:

1. The Wigner equation corresponding (2.2) is

$$
\begin{aligned}
\frac{\partial W_\varepsilon^s}{\partial t} + k \frac{\partial W_\varepsilon^s}{\partial x} &= \frac{1}{\mathrm{i}\varepsilon} \sum_{\mu \in L^*} \mathrm{e}^{\mathrm{i}\mu x/\varepsilon} \hat{V}(\mu) \left[W_\varepsilon^s\left(x, k - \frac{\mu}{2}\right) - W_\varepsilon^s\left(x, k + \frac{\mu}{2}\right) \right] \quad (3.9) \\
&\quad + \frac{1}{\mathrm{i}\varepsilon} \int_\mathbb{R} \frac{\mathrm{d}\omega}{2\pi} \mathrm{e}^{\mathrm{i}\omega x} \hat{U}(\omega) \left[W_\varepsilon^s\left(x, k - \frac{\varepsilon\omega}{2}\right) - W_\varepsilon^s\left(x, k + \frac{\varepsilon\omega}{2}\right) \right].
\end{aligned}
$$

12

2. Corresponding to the asymptotic Wigner equation for asymmetrical transformation (2.6), one has:

$$\frac{\partial W_\varepsilon^s}{\partial t} + k\frac{\partial W_\varepsilon^s}{\partial x} - \frac{\partial U}{\partial x}\frac{\partial W_\varepsilon^s}{\partial k} = -\frac{1}{\varepsilon}\mathcal{L}^s W_\varepsilon^s, \tag{3.10}$$

where the skew symmetric operator $\mathcal{L}^s$ is given by

$$\mathcal{L}^s f(z, k) = k\frac{\partial f}{\partial z} - \frac{1}{i}\sum_{\mu \in L^*} e^{i\mu x/\varepsilon}\hat{V}(\mu)\left[f(x, k - \mu/2) - f(x, k + \mu/2)\right].$$

3. Corresponding to (2.8), one has the $\mathcal{O}(\frac{1}{\varepsilon})$ and $\mathcal{O}(1)$ expansions:

$$\mathcal{L}^s W_0^s = 0, \tag{3.11a}$$

$$\frac{\partial W_0^s}{\partial t} + k\frac{\partial W_0^s}{\partial x} - \frac{\partial U}{\partial x}\frac{\partial W_0^s}{\partial k} = -\mathcal{L}^s W_1^s. \tag{3.11b}$$

4. Same as in (2.13), one has the following symmetrical definition for Q_{mm}

$$Q_{mn}^s(z, k) = Q_{mn}^s(z, \mu, p) = \int_0^{2\pi}\frac{dy}{2\pi}e^{i(p+\mu)y}\Psi_m\left(z - \frac{y}{2}, p\right)\bar{\Psi}_n\left(z + \frac{y}{2}, p\right). \tag{3.12}$$

They are eigenfunctions of $\mathcal{L}^s$

$$\mathcal{L}^s Q_{mn}^s = i(E_m - E_n)Q_{mn}^s. \tag{3.13}$$

5. If the eigenvalues $\{E_n\}$ are well separated, i.e. $E_m \neq E_n$, for $m \neq n$, the solution to (3.11a) is:

$$W_0^s = \sum_m \sigma_{mm}^s Q_{mm}^s. \tag{3.14}$$

By taking the inner product with Q_{mm}^s on both sides of (3.11b), one obtains the same classical Liouville equations for σ_{mm}^s as in (2.21)

$$\partial_t\sigma_{mm}^s + \partial_p E_m\partial_x\sigma_{mm}^s - \partial_x U\partial_p\sigma_{mm}^s = 0. \tag{3.15}$$

6. If some bands touch at point p_c, the solution to (3.10) is given by:

$$W_\varepsilon^s = \sum_m \sigma_{mm}Q_{mm}^s + \sum_{m \neq n}\sigma_{mn}Q_{mn}^s. \tag{3.16}$$

In the two-band case, $m, n = 1, 2$, then σ_{mn}^s is governed by,

$$\partial_t\boldsymbol{\sigma}^s + A^s\partial_x\boldsymbol{\sigma}^s + B^s\partial_p\boldsymbol{\sigma}^s = -B^s C^s\boldsymbol{\sigma}^s + \frac{iD^s}{\varepsilon}\boldsymbol{\sigma}^s, \tag{3.17}$$

13

where $\boldsymbol{\sigma}^s = (\, \sigma_{11}^s \ \sigma_{12}^s \ \sigma_{21}^s \ \sigma_{22}^s \,)^T$, then $B^s = B$, $C^s = C$ and $D^s = D$ are the same as the asymmetric case, while A^s is given by

$$
A^s = \begin{bmatrix}
\partial_p E_1 & \frac{1}{2}\psi_{12} & \frac{1}{2}\psi_{21} & 0 \\
\frac{1}{2}\psi_{21} & \partial_p \frac{E_1+E_2}{2} & 0 & \frac{1}{2}\psi_{21} \\
\frac{1}{2}\psi_{12} & 0 & \partial_p \frac{E_1+E_2}{2} & \frac{1}{2}\psi_{12} \\
0 & \frac{1}{2}\psi_{12} & \frac{1}{2}\psi_{21} & \partial_p E_2
\end{bmatrix}
$$

and ψ_{mn}, ϕ_{mn} are given by (3.2f). Noted that $A^s = (A^s)^\dagger$.

We call this new system obtained by the symmetric Wigner transform (3.17) the Liouville-S system. Apparently the only difference from Liouville-A lies in the transport matrices $A \neq A^s$. But they share the same weak limit as $\varepsilon \to 0$ (see Appendix B for detail). This formally suggests the similar behavior of σ_{11}, σ_{22} and σ_{11}^s, σ_{22}^s, which is confirmed by numerical results in Section 5.1.

4 A multiscale domain decomposition method

4.1 Asymptotic behavior of the two-band semi-classical Liouville systems

Away from p_c, E_1 and E_2 are well-separated, and the $\frac{i}{\varepsilon}$ terms for the transition coefficients σ_{12} and σ_{21} in Liouville-A/S lead to high oscillations, thus as $\varepsilon \to 0$, the system formally goes to its weak limit: the classical one (2.21).

For $\varepsilon > 0$, around p_c, however, both σ_{12} and σ_{21} become significant, and the band-to-band transition is no longer negligible.

In fact, based on the distance to the crossing point p_c, one could obtain some asymptotic properties of the transition coefficients $\sigma_{mn}(m \neq n)$.

Assume that the initial data for the transition coefficients are all zero, and that U_x does not change sign in time for all x, take $-U_x > 0$ for example, then:

Case 1. If $p \ll -C_0\sqrt{\varepsilon}$ for $C_0 = \mathcal{O}(1)$, then σ_{12} and σ_{21} are of $o(\sqrt{\varepsilon})$;

Case 2. If $-C_0\sqrt{\varepsilon} < p < C_0\sqrt{\varepsilon}$, then σ_{12} and σ_{21} are of $\mathcal{O}(\sqrt{\varepsilon})$, and σ_{12} and σ_{21} are slowly varying, i.e. $\partial_t \sigma_{12} \ll \mathcal{O}\left(\frac{1}{\varepsilon}\right)$, and $\partial_t \sigma_{21} \ll \mathcal{O}\left(\frac{1}{\varepsilon}\right)$;

Case 3. If $p \gg C_0\sqrt{\varepsilon}$, σ_{12} and σ_{21} are highly oscillatory with mean 0.

We leave the justification for a simpler model problem to Appendix B.

Remark 4.1. The assumption $\sigma_{mn}(t = 0) = 0$ $(m \neq n)$ is a reasonable assumption. In fact, given arbitrary initial condition, one could check that away from p_c, the weak limit of σ_{mn} is always zero, as $\varepsilon \to 0$, as can be seen in Appendix B. So numerically we treat the initial data for both σ_{12} and σ_{21} zero, given the initial velocity $\partial_x S_0(x)$ away from the crossing point, i.e.

$$\boldsymbol{\sigma}(0, x, p) \approx \delta\left(p - \partial_x S_0(x)\right) \begin{pmatrix} a_1^2 & 0 & 0 & a_2^2 \end{pmatrix}^T, \quad \text{if } \partial_x S_0(x) \neq p_c. \tag{4.1}$$

This assumption is intuitive and empirical, but it does give us some convenience in solving the Liouville-A/S numerically. In fact, the numerical examples provided in Section 5 indeed show that the band-to-band transition is captured very well with initial data (4.1).

4.2 A domain decomposition method

Clearly, one has several observations in hand:

- the classical Liouville is an approximation (in weak limit) to Liouville-A away from the crossing point;

- σ_{12} and σ_{21} are slowly varying in a neighborhood of $p_c = 0$, with a small amplitude before the characteristic hitting p_c, and a rapid oscillation after that.

These observations motivate a domain decomposition method in p-space. The idea is, away from p_c, when the classical Liouville equation (2.21) is a good approximation, we solve this set of equations, and then switch back to Liouville-A when the approximation breaks down around p_c (in the $O(\varepsilon)$ neighborhood of p_c). The gain is obvious: numerically it is much easier and more efficient to solve the classical one, thus this approach saves a great amount of computational cost than solving Liouville-A everywhere. Based on the asymptotic properties of the transition coefficients, we propose the following:

Given a fixed spatial point x, the sign of $-U_x$ determines the traveling direction of wave in p. Assume $-U_x > 0$, i.e. the wave we study is right-going:

Classical regions: $p < -C_0\sqrt{\varepsilon}$ and $p > C_0\sqrt{\varepsilon}$: In this region, coarse mesh independent on ε is used to solve the classical Liouville system (2.21), and σ_{12} and σ_{21} are set to be zero.

Semi-classical region: $p \in B \backslash \{$Classical region$\}$: Solve Liouville-A. The incoming boundary conditions for σ_{12} and σ_{21} are set to be zero, and the incoming boundary condition for σ_{11} and σ_{22} are the inflow boundary condition. A fine mesh is used with Δx and Δt much less than $\sqrt{\varepsilon}$.

In case of $-U_x < 0$, and the wave if left-going, boundary condition can be set up in the same way.

Remark 4.2. Our analysis is based on the regularity of the coefficient matrix C in Liouville-A. But usually, the value of C's element can be of $\mathcal{O}(1/\delta)$ where $\delta = \min_p |E_1(p) - E_2(p)|$ is the minimal band gap. So C will be large if the minimal band gap δ is small, and the numerical discretization in the semi-classical region should resolve this small parameter δ. In the interested regime $\varepsilon \sim \delta^2$, $o(\sqrt{\varepsilon})$ mesh is enough.

5 Numerical examples

In this section we solve the Liouville-A and Liouville-S numerically. Firstly in Section 5.1, we present a numerical method for the equation with a linear external potential $U(x)$. In this special case, we provide an efficient solver without using the domain decomposition method. In Section 5.2, the domain decomposition method is applied for general $U(x)$.

For both examples, we use the Mathieu model, i.e. the periodic potential is $V(z) = \cos z$. The first eight Bloch eigenvalues are shown in Figure 5.1. Apparently, some eigenvalues get

(a)   (b)
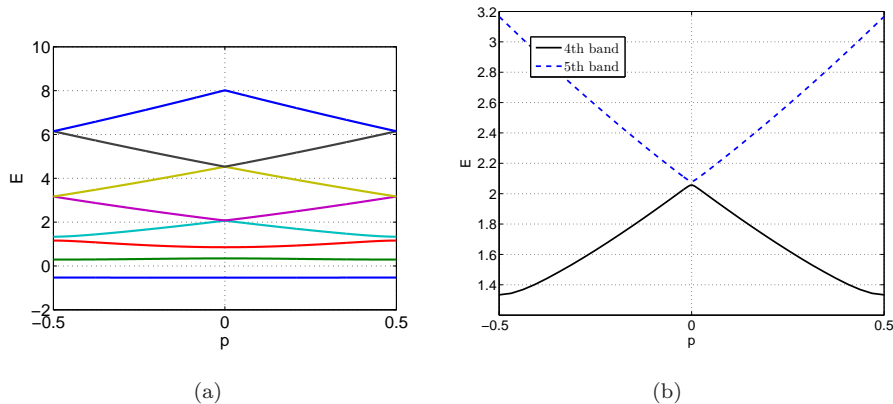
Figure 5.1: The eigenvalues of the Mathieu Model, $V(x) = \cos x$.

very close to each other around $p = 0, \pm 0.5$.

We will focus on the 4th and 5th bands[1]. Denote Ψ_1 and Ψ_2 as the Bloch functions corresponding to the 4th and 5th bands respectively.

For comparison, we will compare the numerical results to the ones given by the original Schrödinger equation, computed through the methods given in [14] with mesh size and time step much smaller than ε.

5.1 Linear $U(x)$

We deal with the linear external potential in this section:

$$U(x) = U_0 - \beta x.$$

Then the Schrödinger equation is:

$$i\varepsilon \phi_t^\varepsilon = -\frac{\varepsilon^2}{2}\phi_{xx}^\varepsilon + \left[\cos\left(\frac{x}{\varepsilon}\right) + (U_0 - \beta x)\right]\phi^\varepsilon, \tag{5.1}$$

with the initial data given as a wave packet along the 4th band:

$$\phi_I = a_0(x)\,\Phi_1\left(\frac{x}{\varepsilon}, \partial_x S_0(x)\right)\,e^{iS_0(x)/\varepsilon}, \text{ with } S_0(x) = p^* x. \tag{5.2}$$

Correspondingly, the Liouville-A becomes:

$$\partial_t \boldsymbol{\sigma} + \beta\partial_p \boldsymbol{\sigma} = \mathcal{R}\boldsymbol{\sigma}, \tag{5.3a}$$

$$\boldsymbol{\sigma}(0, x, p) = \boldsymbol{\sigma}_I(x, p) = |a_0(x)|^2\delta\left(p - \partial_x S_0(x)\right)\begin{pmatrix} 1 & 0 & 0 & 0 \end{pmatrix}^T, \tag{5.3b}$$

with $\mathcal{R}$ given by:

$$\mathcal{R} = -\beta C + \frac{iD}{\varepsilon} - A\partial_x. \tag{5.4}$$

One encounters two computational challenges here. Firstly, one needs to numerically resolve the rapid oscillation. We will present an efficient way to overcome this difficulty by following the characteristics in Section 5.1.1. Secondly, the initial data contains a delta function. Usually one uses a Gaussian function with small variance to approximate it, and the error is related to this variance. As will be discussed in Section 5.1.2, in some special cases, this can be avoided by using the singularity decomposition idea of [15].

Remark 5.1. Here we only discuss Liouville-A. Liouville-S can be computed similarly.

---

[1]The minimum gap between the 4th and 5th bands is 0.0247, located at $p = 0$. The gap is considered small enough so that the quantum effect can be seen for the ε being used.

5.1.1 A Fourier transform based integration method

Let the Fourier transform of $f(t, x, p)$ with respect to x be

$$\hat{f}(t, \eta, p) = \int_{\mathbb{R}} e^{-i\eta x} f(t, x, p) dx.$$

Taking this transform on Liouville-A (5.3a), one gets:

$$\partial_t \hat{\boldsymbol{\sigma}} + \beta \, \partial_p \hat{\boldsymbol{\sigma}} = \left(-\beta C + \frac{iD}{\varepsilon} - i\eta A \right) \hat{\boldsymbol{\sigma}} =: \hat{\mathcal{R}} \hat{\boldsymbol{\sigma}} \qquad (5.5)$$

In this special case, β is a constant so the characteristic line can be obtained analytically. and consequently one can avoid using the mesh thus removes the difficulty due to the high oscillation introduced by the term $\frac{iD}{\varepsilon}$, as will be clear in the following. We take the first time step $t \in [0, \Delta t]$ for example. Along the characteristic line $p(t) = p_0 + \beta t$, one evaluate $\hat{\boldsymbol{\sigma}}$ and $\hat{\mathcal{R}}$ at $(t, p(t), \eta)$ and has:

$$\frac{d\hat{\boldsymbol{\sigma}}}{dt} = \hat{\mathcal{R}} \, \hat{\boldsymbol{\sigma}}. \qquad (5.6)$$

Solution to this ODE system satisfies

$$\hat{\sigma}_{11}(t) = \hat{\sigma}_{11}(0) - \int_0^t i\eta \, \partial_p E_1 \, \hat{\sigma}_{11}(t) dt + \int_0^t \left(\beta(\phi_{12}\hat{\sigma}_{12} - \phi_{21}\hat{\sigma}_{21}) - i\eta \, \psi_{12}\hat{\sigma}_{12} \right) dt, \quad (5.7a)$$

$$\hat{\sigma}_{12}(t) = e^{\int_0^t K^\varepsilon(\tau)d\tau} \hat{\sigma}_{12}(0) + \int_0^t e^{\int_s^t K^\varepsilon(\tau)d\tau} \left(G(s)\hat{\sigma}_{11}(s) - H(s)\hat{\sigma}_{22}(s) \right) ds, \qquad (5.7b)$$

where:

$$K^\varepsilon = \frac{i}{\varepsilon}(E_2 - E_1) - i\eta \, \partial_p E_2 - \beta(\phi_{11} - \phi_{22}), \qquad G = -\beta\bar{\phi}_{12} - i\eta\psi_{21}, \qquad H = \beta\bar{\phi}_{12}.$$

For t small. an approximation to (5.7) is

$$\hat{\sigma}_{11}(t) \approx \hat{\sigma}_{11}(0) - i\eta t \partial_p E_1\big(p(t)\big) \hat{\sigma}_{11}(t)$$
$$+ \big(\beta\phi_{12}(0) - i\eta\psi_{12}(0)\big) \int_0^t \hat{\sigma}_{12} dt - \beta\phi_{21}(0) \int_0^t \hat{\sigma}_{21} dt, \qquad (5.8a)$$

$$\hat{\sigma}_{12}(t) \approx \hat{\sigma}_{12}(0) e^{\int_0^t K^\varepsilon(\tau)d\tau}$$
$$+ \big(G(0)\hat{\sigma}_{11}(0) - H(0)\hat{\sigma}_{22}(0)\big) \int_0^t e^{\int_s^t K^\varepsilon(\tau)d\tau} ds. \qquad (5.8b)$$

Plug (5.8b) into (5.8a), to evaluate $\hat{\sigma}_{11}(\Delta t)$ and $\hat{\sigma}_{12}(\Delta t)$, one needs to compute:

$$F_0 := e^{\int_0^t K^\varepsilon(\tau)d\tau}, \quad F_1 := \int_0^{\Delta t} e^{\int_0^t K^\varepsilon(\tau)d\tau} \, dt, \quad \text{and} \quad F_2 := \int_0^{\Delta t} \int_0^t e^{\int_s^t K^\varepsilon(\tau)d\tau} \, ds \, dt.$$
$$(5.9)$$

However, to compute F_0, F_1 and F_2 is not easy since their integrands are highly oscillatory. But if one chooses $|\beta|\Delta t = \Delta p$, then at each time step one follows exactly the characteristics,

so $p(t)$ always lie on the grid points, thus F_0, F_1 and F_2 are *time independent*, and one only needs to compute them *once* (with a highly resolved calculation). Similar analysis can be carried out for $\hat{\sigma}_{21}$ and $\hat{\sigma}_{22}$.

We prove the stability of this method by using it on a simpler model problem, and it will be justified in Appendix C.

5.1.2 A singularity decomposition idea

To handle the delta function in the initial condition (5.3b), one usually approximates it with a Gaussian function with small variance, and numerical error was determined by the width of the Gaussian. As stated before, in some special cases, this error could be avoided, and the example we are discussing here is for when $\partial_x S_0(x) \equiv p^* = const$, for which, we apply the singularity decomposition method introduced in [15] to reduce the error. Write the ansatz of $\hat{\boldsymbol{\sigma}}_{mn}(t, x, p)$ as:

$$\boldsymbol{\sigma}(t, x, p) = \boldsymbol{\omega}(t, x, p)\, \delta\big(\theta(t, p)\big) \tag{5.10}$$

in which:

- $\theta(t, p) = p - (p^* + \beta t)$, which solves the Liouville equation

$$\partial_t \theta + \beta\, \partial_p \theta = 0\,,$$

- $\boldsymbol{\omega}$ satisfies the same equation as $\boldsymbol{\sigma}$:

$$\partial_t \boldsymbol{\omega} + \beta\, \partial_p \boldsymbol{\omega} = \mathcal{R}\boldsymbol{\omega}\,. \tag{5.11}$$

These can be proved by simple derivations. Formally, one has

$$
\begin{aligned}
\frac{\partial \boldsymbol{\sigma}}{\partial t} &= \frac{\partial}{\partial t}\big(\boldsymbol{\omega}\,\delta(\theta)\big) = \frac{\partial \boldsymbol{\omega}}{\partial t}\,\delta(\theta) + \boldsymbol{\omega}\,\delta'(\theta)\frac{\partial \theta}{\partial t} \\
&= \mathcal{R}\boldsymbol{\omega}\,\delta(\theta) - \beta\frac{\partial \boldsymbol{\omega}}{\partial p}\,\delta(\theta) - \beta\boldsymbol{\omega}\,\delta'(\theta) \\
&= \mathcal{R}\boldsymbol{\omega}\,\delta(\theta) - \beta\frac{\partial \boldsymbol{\omega}}{\partial p}\,\delta(\theta) - \beta\boldsymbol{\omega}\,\delta'(\theta)\frac{\partial \theta}{\partial p} \\
&= \mathcal{R}\boldsymbol{\omega}\,\delta(\theta) - \beta\frac{\partial}{\partial p}\big(\boldsymbol{\omega}\,\delta(\theta)\big) \\
&= \mathcal{R}\boldsymbol{\sigma} - \beta\frac{\partial \boldsymbol{\sigma}}{\partial p}\,.
\end{aligned}
$$

The equalities above should be understood in the distributional sense. The decomposition (5.10) enables one to solve for $\boldsymbol{\omega}$ and θ separately with good (bounded) initial data $|a_0(x)|^2$

and $\partial_x S_0(x)$ respectively. The equation $\boldsymbol{\omega}$ satisfies is the same as the one for $\boldsymbol{\sigma}$, thus the numerical method introduced in Section 5.1.1 can be used. In the final output, one needs to get back to $\boldsymbol{\sigma}$ using (5.10), so a discrete delta approximation is only needed at the output time, not during time evolution.

5.1.3 Numerical experiments

We show the numerical results of the Liouville-A/S with the following data

$$\beta = 1, \qquad p^* = -0.25, \qquad a_0(x) = \exp\left(-\frac{25(x-\pi)^2}{2}\right). \tag{5.12}$$

We compute the density, the cumulative density function (c.d.f.) and mass in the 1st band, defined respectively by:

$$\rho^\varepsilon = |\phi^\varepsilon|^2, \qquad \gamma^\varepsilon = \int_{-\infty}^x \rho^\varepsilon(y)dy, \qquad m_1(t) = \int |\mathbb{P}_1\phi^\varepsilon(t,x)|^2 dx, \tag{5.13}$$

where $\mathbb{P}_n$ is the projection onto the nth band:

$$\mathbb{P}_n\phi(x) = \int_B dp \int_\mathbb{R} dy \phi(y)\bar{\Psi}_n(y,p)\Psi_n(x,p), \quad \phi \in L^2(\mathbb{R}),\ m \in \mathbb{N}.$$

The two integrals in (5.13) are calculated by the midpoint quadrature rule numerically.

Figure 5.2 shows the density and c.d.f. computed for the Schrödinger equation, the Liouville-A and the Liouville-S respectively at $t = 0.5$. The results match quite well.

Figure 5.3 shows the evolution of m_1 as a function of time t. One can see the total mass on the first band jumps down at around $t = 0.25$, when the momentum p reaches $p_c = 0$, reflecting the 4th-to-5th band transition. The experiment also shows that smaller ε gives smaller transition rate. Note that some small oscillations occur around the crossing region. They are related to the interference phenomena, and are usually called the Stueckelberg oscillation [5, 27, 29].

Define L^1 error in the cumulative distribution function (c.d.f.) [11, 17]:

$$\mathrm{Err}^\varepsilon(t) = \int_\mathbb{R} \left| \int_{-\infty}^x \left(\rho_S^\varepsilon(t,z) - \rho_L^\varepsilon(t,z)\right)dz \right| dx, \tag{5.14}$$

where ρ_S^ε and ρ_L^ε denote the density calculated by the Schrödinger equation and the Liouville system respectively. Numerically we compute (5.14) using the midpoint quadrature rule. Figure 5.4 shows this at time $t = 0.5$. As $\varepsilon \to 0$, the Liouville system gets more accurate, and the error decreases with the speed of $\mathcal{O}(\varepsilon)$.
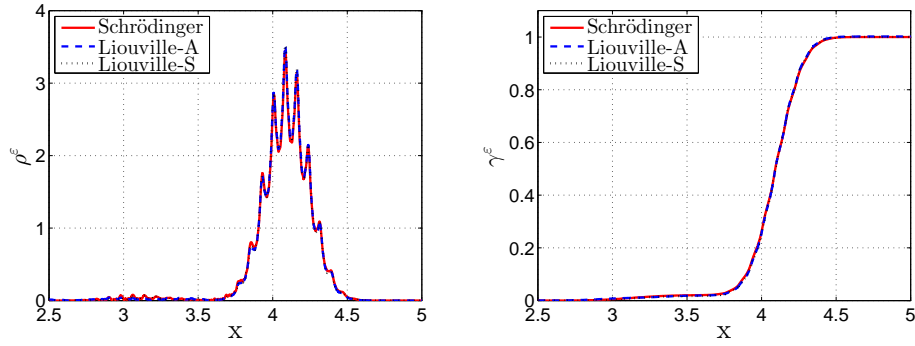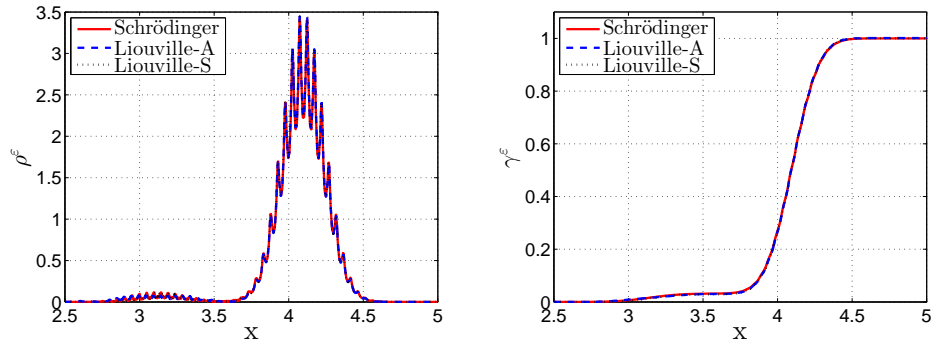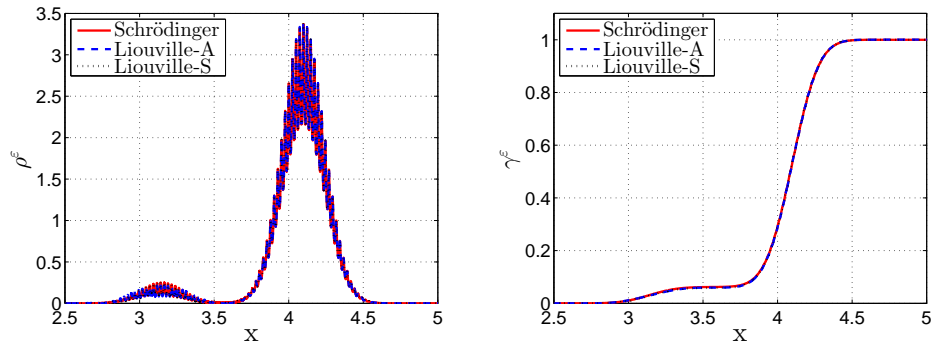
Figure 5.2: The example in Sec. 5.1.3, $t = 0.5$. The left and right column are for the position density ρ^ε, and c.d.f. γ^ε respectively. The solid line, the dash line and the dotted line are the numerical solutions to the Schrödinger, the Liouville-A and the Liouville-S respectively.

(a) $\varepsilon = 2^{-8}$

(b) $\varepsilon = 2^{-9}$

(c) $\varepsilon = 2^{-10}$

(d) $\varepsilon = 2^{-11}$
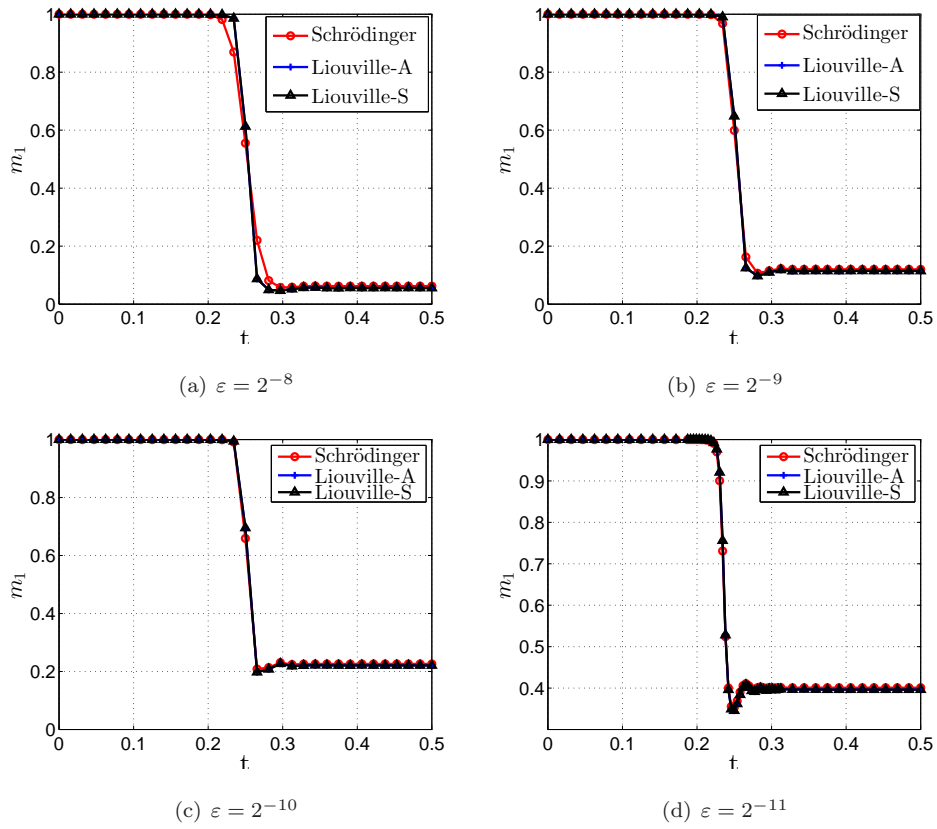
Figure 5.3: The example in Sec. 5.1.3 : time evolution of $m_1(t)$ defined in (5.13).
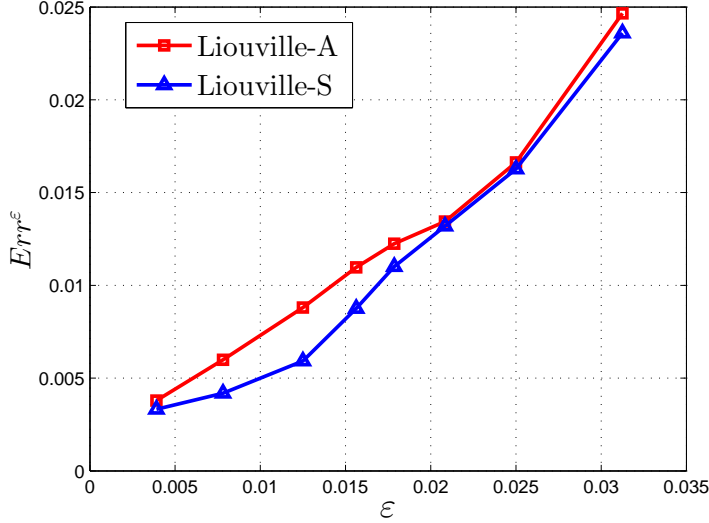
Figure 5.4: The example in Sec. 5.1.3 : Err^ε as function of ε at $t = 0.5$.

5.2 A domain decomposition computation

This section shows examples with varying U_x. For this general case, the p-characteristic is no longer a straight line, and the fast solver in the previous section is no longer valid. To numerically solve Liouville-A, we use the domain decomposition method. The classical finite volume method is used for the convection terms.

We compute the Liouville-A system with both a pure and a mixed state initial data with:

$$U(x) = -\frac{x - \sin x}{2} .$$

5.2.1 A pure state initial data

In this example, we use the same pure state initial data as in the previous example (5.2),(5.12). Correspondingly, the initial data for the Liouville-A system is given by (5.3b). Numerically a Gaussian function centered at p^* with variance of $\varepsilon/16$ is used to approximate the $\delta-$function.

Figures 5.5 and 5.6 show the density, the c.d.f at $t = 0.5$ and evolution of m_1 (5.13) computed for both the Schrödinger equation and the Liouville-A system. The numerical results for the two systems agree well. Figure 5.7 gives decay of Err^ε (5.14). The numerical results show that the hybrid model can capture the band-to-band transition phenomena,
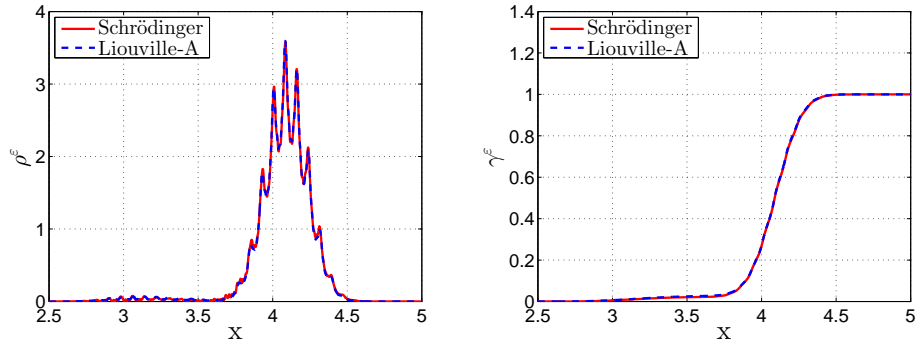
(a) $\varepsilon = \frac{1}{80}$
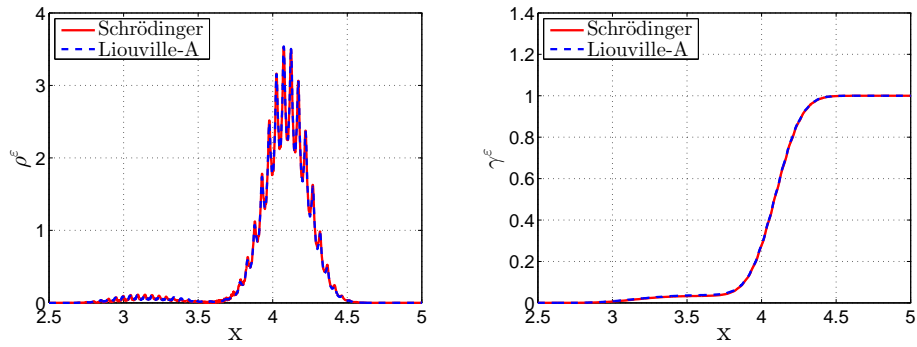
(b) $\varepsilon = \frac{1}{128}$
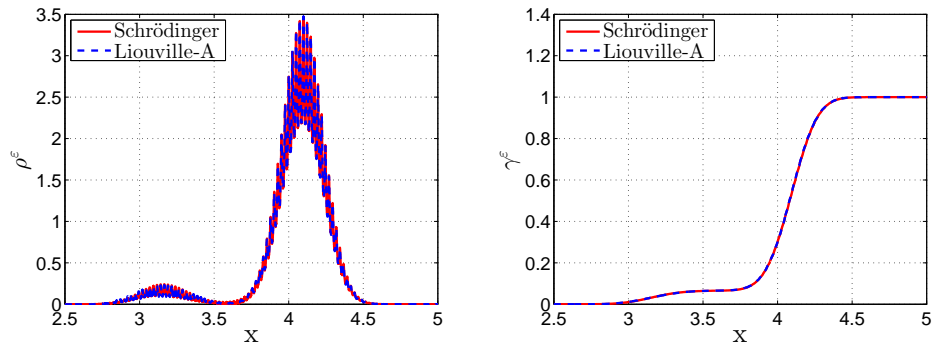
(c) $\varepsilon = \frac{1}{256}$

Figure 5.5: The example in Sec. 5.2.1. $t = 0.5$. The left and right columns show the position density ρ^ε, and the c.d.f. γ^ε respectively.

(a) $\varepsilon = 2^{-8}$

(b) $\varepsilon = 2^{-9}$

(c) $\varepsilon = 2^{-10}$

(d) $\varepsilon = 2^{-11}$
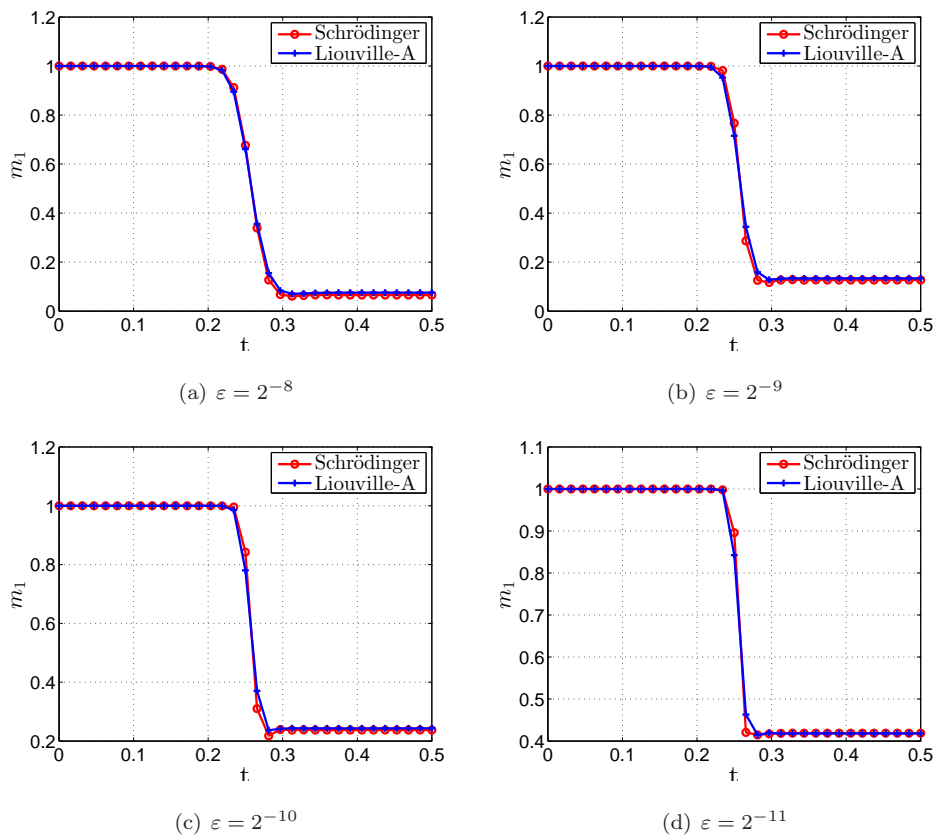
Figure 5.6: The example in Sec. 5.2.1: time evolution of $m_1(t)$ defined in (5.13).
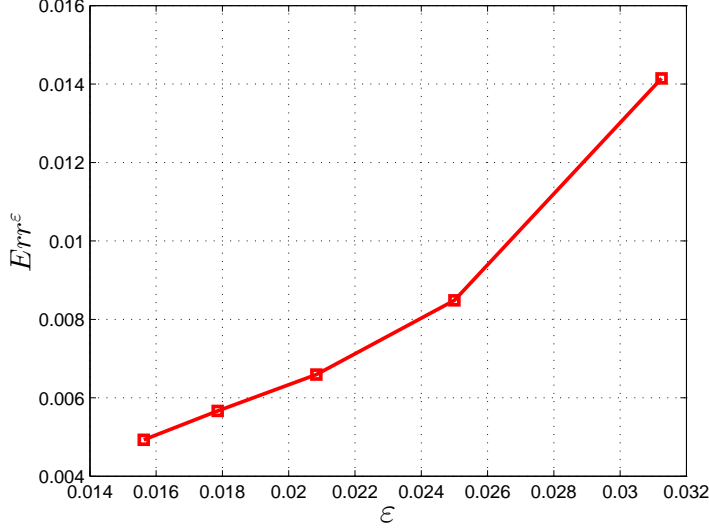
Figure 5.7: The numerical example in Sec. 5.2.1: the L^1 error Err^ε between Liouville-A and the Schrödinger solution at $t = 0.5$.

and the error decays like $\mathcal{O}(\varepsilon)$.

Remark 5.2. As U_x varies with x, the wave packet becomes decoherent. This weakens the interference phenomenon [5, 27, 29]. As one can see in Figure 5.6, the Stueckelberg oscillations around the crossing region is much weaker than those in the previous example.

5.2.2 A mixed state initial data.

This example is for the case when the initial data is a mixed state:

$$\phi_I = a_0(x) \left[\Phi_1 \left(\frac{x}{\varepsilon}, p^* \right) e^{ip^* x/\varepsilon} + \Phi_2 \left(\frac{x}{\varepsilon}, p^* \right) e^{ip^* x/\varepsilon} \right], \quad p^* = -0.25.$$

Correspondingly, the initial data for the semi-classical Liouville system should be:

$$\boldsymbol{\sigma} = a_0^2(x) \, \delta(p - p^*) \, [1, 1, 1, 1]^T \, .$$

Since p^* is away from the crossing point and σ_{12} and σ_{21} weakly converge to zero as $\varepsilon \to 0$, numerically, we regard them as zero and use

$$\boldsymbol{\sigma} \approx a_0^2(x) \, \delta_G(p - p^*) \, [1, 0, 0, 1]^T$$

as the initial condition, where $\delta_G(p)$ is a Gaussian function centered at zero.

The density and the c.d.f. are computed for the Liouville-A and the Schrödinger, compared in Figure 5.8. Err$^\varepsilon$ as a function of ε is shown in Figure 5.9.

6   Conclusion

In this paper we derive semiclassical models for the linear Schrödinger equation with periodic potentials. These models take into account the band corssing, which is important to describe quantum transitions between different Bloch bands. Away from the band-crossing zones these models reduce (in the sense of weak limit) to the classical Liouville system for each Bloch band. We also couple these semiclassical models (to be used near the corssing zones) and the classical Liouville equation (used away from the crossing zones) for an efficient multiscale computation. Our numerical experiments show that these semiclassical models provide correct quantum transitions near the crossing zones when compared with the direct simulation of the original Schrödinger equation.
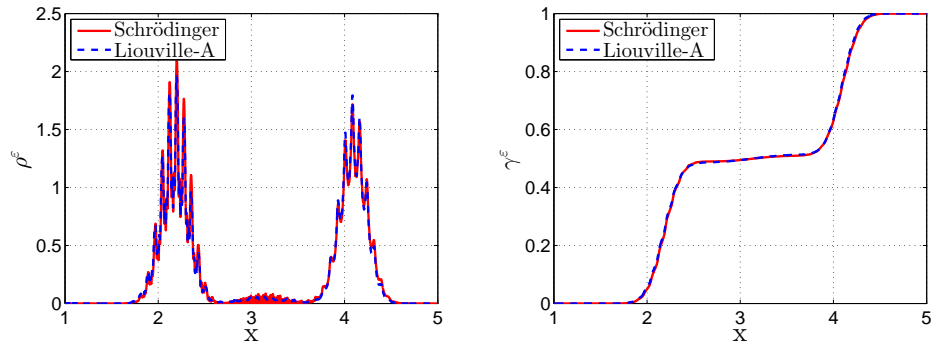
(a) $\varepsilon = \frac{1}{80}$
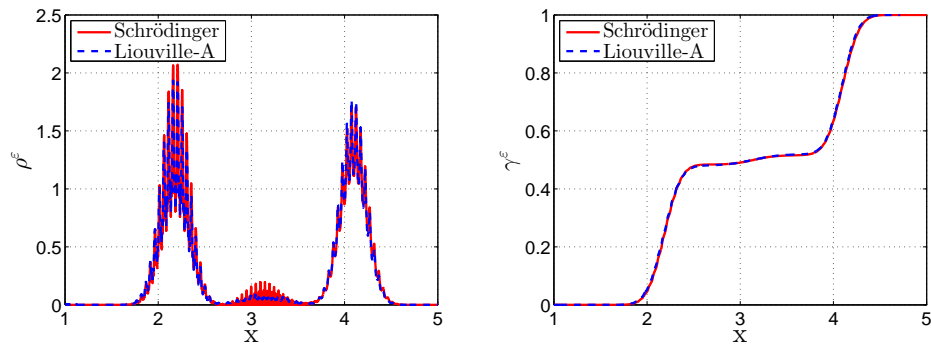
(b) $\varepsilon = \frac{1}{128}$
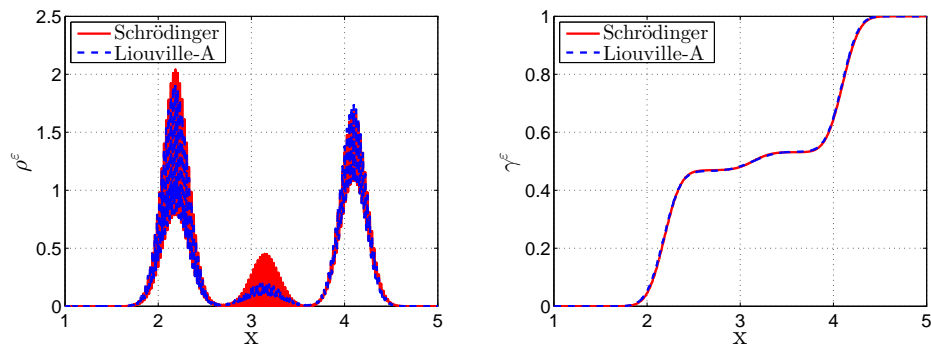
(c) $\varepsilon = \frac{1}{256}$

Figure 5.8: The example in Sec. 5.2.2: at time $t = 0.5$. The left and the right columns show the position density ρ^ε, and the c.d.f. γ^ε respectively.
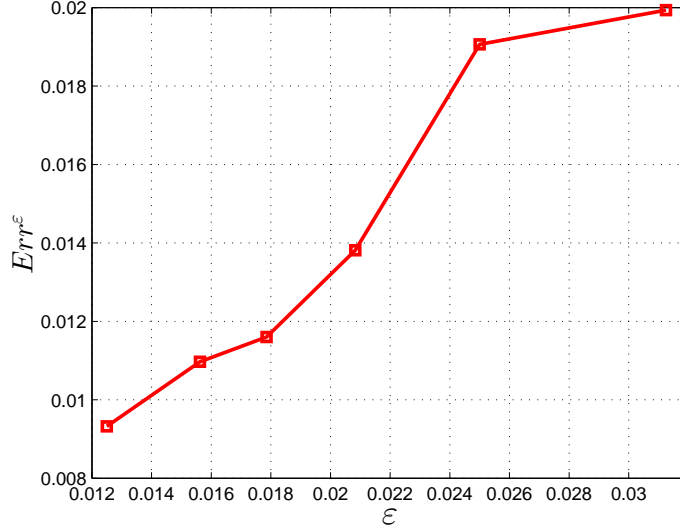
Figure 5.9: The numerical example in Sec. 5.2.2: the L^1 error Err^ε as a function of ε at $t = 0.5$.

Appendices

A   Hyperbolicity of the two-band semi-classical Liouville systems

The semi-classical Liouville system (Liouville-A) is

$$\partial_t \boldsymbol{\sigma} + A\partial_x \boldsymbol{\sigma} - U_x \partial_p \boldsymbol{\sigma} = S\boldsymbol{\sigma} \tag{A.1}$$

where

$$S = C + \frac{\mathrm{i}D}{\varepsilon} \ ,$$

and $\boldsymbol{\sigma}$, A, C, D are defined in (3.2). Noted that $A = A^\dagger$ and $S = -S^\dagger$. To check the hyperbolicity, we separate the real and imaginary parts.

$$\boldsymbol{\sigma} = \mathrm{Re}\,\boldsymbol{\sigma} + \mathrm{i}\,\mathrm{Im}\,\boldsymbol{\sigma},$$

$$A = \mathrm{Re}\,A + \mathrm{i}\,\mathrm{Im}\,A,$$

$$S = \mathrm{Re}\,S + \mathrm{i}\,\mathrm{Im}\,S,$$

29

with $\operatorname{Re} F$ and $\operatorname{Im} F$ denoting the real part and imaginary part of F respectively. Then one can get

$$\begin{bmatrix} \operatorname{Re}\boldsymbol{\sigma} \\ \operatorname{Im}\boldsymbol{\sigma} \end{bmatrix}_t + \begin{bmatrix} \operatorname{Re}A & -\operatorname{Im}A \\ \operatorname{Im}A & \operatorname{Re}A \end{bmatrix}\begin{bmatrix} \operatorname{Re}\boldsymbol{\sigma} \\ \operatorname{Im}\boldsymbol{\sigma} \end{bmatrix}_x + U_x \begin{bmatrix} \operatorname{Re}\boldsymbol{\sigma} \\ \operatorname{Im}\boldsymbol{\sigma} \end{bmatrix}_p = \begin{bmatrix} \operatorname{Re}S & -\operatorname{Im}S \\ \operatorname{Im}S & \operatorname{Re}S \end{bmatrix}\begin{bmatrix} \operatorname{Re}\boldsymbol{\sigma} \\ \operatorname{Im}\boldsymbol{\sigma} \end{bmatrix} \tag{A.2}$$

Since $A = A^\dagger$, then $\operatorname{Re}A = \operatorname{Re}A^T$, $\operatorname{Im}A = -\operatorname{Im}A^T$. Thus have that the matrix

$$\begin{bmatrix} \operatorname{Re}A & -\operatorname{Im}A \\ \operatorname{Im}A & \operatorname{Re}A \end{bmatrix}$$

is a symmetric matrix, which implies the hyperbolicity of the system.

In addition, since $S = -S^\dagger$, then $\operatorname{Re}S = -\operatorname{Re}S^T$, $\operatorname{Im}S = \operatorname{Im}S^T$. Therefore the matrix

$$\begin{bmatrix} \operatorname{Re}S & -\operatorname{Im}S \\ \operatorname{Im}S & \operatorname{Re}S \end{bmatrix}$$

is a skew-symmetric matrix.

Similarly, one can obtain the hyperbolicity of system Liouvill-S (3.17).

B Some basic analysis of the semi-classical Liouville systems

To understand the asymptotic behavior of the solution to the Liouville-A system (3.2), as mentioned in Section 4.1, we look at a simpler model system:

$$\begin{cases} \partial_t g + \partial_x f + b(x)\partial_p g = 0, \\ \partial_t f + a(p)\partial_x f + \partial_x g + b(x)\partial_p f = \frac{\mathrm{i}}{\varepsilon}c(p)f, \\ g(0,x,p) = g_I(x,p), \quad f(0,x,p) = f_I(x,p). \end{cases} \tag{B.1}$$

The initial conditions g_I and f_I are bounded smooth functions independent on ε, $b > 0$ and the set of zeros for $c(p)$: $S_c = \{p : c(p) = 0\}$ is measured zero. It is easy to check that (B.1) is a linear hyperbolic system, and the solutions g and f are bounded uniformly in ε [6].

B.1 Weak convergence

We consider the weak limit of the solution of (B.1) in this subsection. To do this, we introduce the inner product $\langle \cdot, \cdot \rangle$ as

$$\langle u, v \rangle = \int_0^\infty \int_{\mathbb{R}^2} u(t,x,p)\bar{v}(t,x,p)\,\mathrm{d}x\,\mathrm{d}p\,\mathrm{d}t.$$

Choose an arbitrary test function $h \in C_0^\infty(\mathbb{R}^+ \times \mathbb{R}^2)$, take the inner product on both side of (B.1) w.r.t h, one gets

$$\begin{cases} \langle \partial_t g, h \rangle - \langle f, \partial_x h \rangle + \langle b\partial_p g, h \rangle = 0, \\ \langle f, \partial_t h \rangle + \langle af, \partial_x h \rangle + \langle g, \partial_x h \rangle + \langle bf, \partial_p h \rangle = -\frac{i}{\varepsilon} \langle cf, h \rangle. \end{cases} \quad \text{(B.2)}$$

The derivatives in the equation of (B.2) are acted on the smooth function h, and the left side is bounded. One gets

$$\langle cf, h \rangle \to 0 \quad \text{as} \quad \varepsilon \to 0 \quad \text{for all } h \in C_0^\infty(\mathbb{R}^+ \times \mathbb{R}^2).$$

Given that c is almost surely nonzero, and f is bounded, one gets

$$f \rightharpoonup 0 \text{ weakly.}$$

Combined with the first equation in (B.2), one gets

$$\partial_t g + b(x)\partial_p g \rightharpoonup 0 \text{ weakly.}$$

B.2 Strong convergence: for constant b

In these two subsections, we formally prove that before getting close to the crossing region, $c(p)$ is assumed to be bigger than a constant c_0 that is unrelated to ε. In this region, f is constantly small and controlled by $\mathcal{O}(\varepsilon)$. This subsection is for the case when the speed on p direction is a constant: $b(x) = \beta$. Along the p-characteristic line $p(t) = p_0 + \beta t$, one applies the Fourier transform to the x-variable, and gets:

$$\frac{\mathrm{d}}{\mathrm{d}t} \boldsymbol{f} = \mathrm{i}R(t)\boldsymbol{f}, \quad \text{(B.3)}$$

where $\boldsymbol{f}(t, \eta) = (\hat{g}(t, \eta, p(t)), \hat{f}(t, \eta, p(t)))^T$ and

$$R(t) = \begin{pmatrix} 0 & -\eta \\ -\eta & c(p(t))/\varepsilon - \eta a(p(t)) \end{pmatrix}.$$

The two eigenvalues of $R(t)$ are both real, and thus the system above has a bounded solution satisfying

$$|\hat{g}(t, \eta)|^2 + |\hat{f}(t, \eta)|^2 = |\hat{g}_I(\eta)|^2 + |\hat{f}_I(\eta)|^2.$$

The equivalence between norms gives:

$$|\hat{g}(t, \eta)| + |\hat{f}(t, \eta)| < C(|\hat{g}_I(\eta)| + |\hat{f}_I(\eta)|). \quad \text{(B.4)}$$

Adopt it into the solution to (B.3), one gets

$$|\partial_t g(t,x)| = \frac{1}{2\pi}\left|\int_{\mathbb{R}} \eta \hat{f}(t,\eta)e^{i\eta x}d\eta\right| \leq \frac{1}{2\pi}\int_{\mathbb{R}}|\eta|\,|\hat{f}(t,\eta)|d\eta \leq C\int_{\mathbb{R}}|\eta|\left(|\hat{g}_I(\eta)|+|\hat{f}_I(\eta)|\right)d\eta$$

$$|\partial_{tx}^2 g(t,x)| = \frac{1}{2\pi}\left|\int_{\mathbb{R}} \eta^2 \hat{f}(t,\eta)e^{i\eta x}d\eta\right| \leq \frac{1}{2\pi}\int_{\mathbb{R}}|\eta|^2\,|\hat{f}(t,\eta)|d\eta \leq C\int_{\mathbb{R}}|\eta|^2\left(|\hat{g}_I(\eta)|+|\hat{f}_I(\eta)|\right)d\eta$$

If the initial conditions $\hat{g}_I$ and $\hat{f}_I$ are smooth enough, and decay fast as $\eta \to \infty$, one could easily get that $\partial_t g(t,x)$ and $\partial_{tx}^2 g(t,x)$ are both bounded in time independent of ε, and thus g and $\partial_x g$ are slowly varying in time.

Remark B.1. In the derivation above, we dropped the $p(t)$-dependence in the functions for simplicity. The partial derivative in the t-variable ∂_t should be understood as taking along the p-characteristic line $p(t)$, i.e. $\partial_t g(t,x) = \partial_t g(t,x,p) + \beta\partial_p g(t,x,p)$.

Assume that $f_I(x) \equiv 0$, one follows the characteristics of $x(t)$ by solving $\dot{x}(t) = a(t,x)$ and gets:

$$f\big(t,x(t),p(t)\big) = -\int_0^t \exp\left(\frac{i}{\varepsilon}\int_{t-s}^t c\,(p(\tau))\,d\tau\right)\frac{\partial g}{\partial x}\big(t-s,x(t-s),p(t-s)\big)\,ds\,.$$

By the assumption, before hitting the crossing region, $c(p(\tau)) > c_0 > 0$, then the stationary phase argument suggests that, given slowly varying $\partial_x g(t,x,p(t))$, $f = \mathcal{O}(\varepsilon)$.

The observations from the above two subsections suggest that $f \rightharpoonup 0$, and before getting close to the crossing region, f is as small as of $O(\varepsilon)$. Based on these arguments, for the Liouville-A system (3.2), and propose the following conjecture: if σ_{12} and σ_{21} are initially zero, then:

Case 1. If $p \ll -\sqrt{\varepsilon}$, then σ_{12} and σ_{21} are of $o(\sqrt{\varepsilon})$;

Case 2. If $p \in [-\sqrt{\varepsilon}, \sqrt{\varepsilon}]$, then σ_{12} and σ_{21} are of $\mathcal{O}(\sqrt{\varepsilon})$, and slowly varying;

Case 3. If $p \gg \sqrt{\varepsilon}$, σ_{12} and σ_{21} are highly oscillatory, and converge to 0 weakly.

C The integration method of a simple model system

In this section, we apply the method in (5.8) onto a simple model to show stability.

$$\frac{d}{dt}\mathbf{f}(t,p_0+t) = R(p_0+t)\,\mathbf{f}(t,p_0+t),$$

where $\mathbf{f}(t,p) = (g(t,p), f(t,p))^T$, $p = p_0 + t$, and

$$R(p) = \begin{pmatrix} r_{11}(p) & r_{12}(p) \\ -\bar{r}_{12}(p) & r_{22}^\varepsilon(p) \end{pmatrix}.$$

with $r_{22}^{\varepsilon}(p) = r_{22}(p) + \frac{i}{\varepsilon}c(p)$, while r_{11} and r_{22} are purely imaginary, and $c(p)$ real and positive. r_{11}, r_{22} and r_{12} are independent on ε.

Set up mesh as $t^j = j\Delta t$, and $p^i = -\frac{1}{2} + (i-1)\Delta p$, with Δp and Δt being the mesh size. Denote g_i^j and f_i^j as the numerical result at (t^j, p^i), then (5.8) gives

$$f(t, p(t)) = f_i^j\, e^{\int_0^t r_{22}^{\varepsilon}(p^i+\tau)d\tau} - g_i^j\, \bar{r}_{12}(p^i) \int_0^t e^{\int_s^t r_{22}^{\varepsilon}(p^i+\tau)d\tau}ds, \tag{C.1a}$$

$$g(t, p(t)) = g_i^j + g(t, p(t))\, r_{11}(p(t)) + r_{12}(p^i) \int_0^t \tilde{f}(t^j + s, p^i + s)\, ds \tag{C.1b}$$

Plug (C.1a) into (C.1b), and evaluate them at (t^{j+1}, p^{i+1}), one obtains:

$$\left(1 - r_{11}(p^{i+1})\Delta t\right) g_{i+1}^{j+1} = g_i^j \left(1 - |r_{12}(p^i)|^2 \int_0^{\Delta t}\int_0^t e^{\int_s^t r_{22}^{\varepsilon}(p^i+\tau)d\tau}ds\, dt\right)$$

$$+ f_i^j\, r_{12}(p^i) \int_0^{\Delta t} e^{\int_0^t r_{22}^{\varepsilon}(p^i+\tau)d\tau}dt\ . \tag{C.2}$$

Written in vector form gives

$$\mathbf{f}_{i+1}^{j+1} = M_i\, \mathbf{f}_i^j, \tag{C.3}$$

with

$$M_i = \begin{pmatrix} \dfrac{1-|r_{12}(p^i)|^2 \int_0^{\Delta t}\int_0^t e^{\int_s^t r_{22}^{\varepsilon}(p^i+\tau)d\tau}ds\,dt}{1-r_{11}(p^{i+1})\Delta t} & \dfrac{r_{12}(p^i)\int_0^{\Delta t} e^{\int_0^t r_{22}^{\varepsilon}(p^i+\tau)d\tau}dt}{1-r_{11}(p^{i+1})\Delta t} \\ -\bar{r}_{12}(p^i) \int_0^{\Delta t} e^{\int_s^{\Delta t} r_{22}^{\varepsilon}(p^i+\tau)d\tau}ds & e^{\int_0^{\Delta t} r_{22}^{\varepsilon}(p^i+\tau)d\tau} \end{pmatrix}.$$

The following quantities in the matrix M_i should be evaluated very accurately:

$$F_0 = e^{\int_0^{\Delta t} r_{22}^{\varepsilon}(p^i+\tau)d\tau}, \qquad F_1 = \int_0^{\Delta t} e^{\int_0^t r_{22}^{\varepsilon}(p^i+\tau)d\tau}dt, \qquad F_2 = \int_0^{\Delta t}\int_0^t e^{\int_s^t r_{22}^{\varepsilon}(p^i+\tau)d\tau}ds\,dt.$$

Since r_{22}^{ε} is purely imaginary, $F_0 = O(1), F_1 = O(\Delta t), F_2 = O((\Delta t)^2)$.

Remark C.1. These three quantities only depend on the mesh grid point index i but not the time steps index j, thus they only need to be computed once at the beginning of the computation.

Given $\varepsilon \ll \Delta t$, the integrands of F_1 and F_2 are highly oscillatory, and one can see that $|F_1| \sim \mathcal{O}(\varepsilon)$ and $|F_2| \sim \mathcal{O}(\varepsilon^2)$. Simple calculation shows that M_i can be written as

$$M_i = \Omega\, \tilde{M}_i,$$

with

$$\Omega = \mathrm{diag}\left(\frac{1}{1 - r_{11}(p^{j+1})\Delta t}, 1\right), \qquad \tilde{M}_i = \begin{pmatrix} 1 - |r_{12}(p^i)|^2\, F_2 & r_{12}\, F_1 \\ -\bar{r}_{12}\, \bar{F}_1 & F_0 \end{pmatrix}.$$

With purely imaginary r_{11} and r_{22}^{ε}, it is easy to prove that $\|\Omega\|_\infty \leq 1$, and $\|\tilde{M}_i\|_\infty \leq (1 + \mathcal{O}(\Delta t))$, and thus $\|M_i\|_\infty \leq (1 + \mathcal{O}(\Delta t))$. This implies asymptotic stability of the scheme (C.3) independent of $\varepsilon \to 0$.

References

[1] G. Bal, A. Fannjiang, G. Papanicolaou, and L. Ryzhik. Radiative transport in a periodic structure. *Journal of Statistical Physics*, 95(1):479–494, 1999.

[2] F. Bloch. Über die quantenmechanik der elektronen in kristallgittern. *Zeitschrift für Physik A Hadrons and Nuclei*, 52(7):555–600, 1929.

[3] A. Bohm, A. Mostafazadeh, H. Koizumi, Q. Niu, and J. Zwanziger. The Geometric Phase in Quantum Systems: Foundations, Mathematical Concepts, and Applications in Molecular and Condensed Matter Physics. *Springer*, 2012.

[4] R. Carles, P.A. Markowich, and C. Sparber. Semiclassical asymptotics for weakly nonlinear Bloch waves. *Journal of Statistical Physics*, 117(1):343–375, 2004.

[5] M.S. Child. Atom-Molecule Collision Theory. *Plenum, New York*, 1979.

[6] R. Courant and D. Hilbert. *Methods of mathematical physics: volume 2*. Wiley India Pvt. Ltd., 2008.

[7] K. Drukker. Basics of surface hopping in mixed quantum/classical simulations. *Journal of Computational Physics*, 153(2):225–272, 1999.

[8] W. E, J. Lu, and X. Yang. Asymptotic analysis of quantum dynamics in crystals: The Bloch-Wigner transform, Bloch dynamics and berry phase. *Acta Mathematicae Applicatae Sinica (English Series)*, pages 1–12, 2011.

[9] Clotilde Fermanian Kammerer and Caroline Lasser. Wigner measures and codimension two crossings. *J. Math. Phys.*, 44(2):507–527, 2003.

[10] P. Gérard, P.A. Markowich, N.J. Mauser, and F. Poupaud. Homogenization limits and Wigner transforms. *Communications on Pure and Applied Mathematics*, 50(4):323–379, 1997.

[11] L. Gosse and N.J. Mauser. Multiphase semiclassical approximation of an electron in a one-dimensional crystalline lattice-III. From ab initio models to WKB for Schrödinger-Poisson. *Journal of Computational Physics*, 211(1):326–346, 2006.

[12] George A. Hagedorn. Molecular propagation through electron energy level crossings. *Mem. Amer. Math. Soc.*, 111(536):vi+130, 1994.

[13] I. Horenko, C. Salzmann, B. Schmidt, and C. Schütte. Quantum-classical Liouville approach to molecular dynamics: Surface hopping Gaussian phase-space packets. *The Journal of Chemical Physics*, 117:11075–11088, 2002.

[14] Z. Huang, S. Jin, P.A. Markowich, and C. Sparber. A Bloch decomposition-based split-step pseudospectral method for quantum dynamics with periodic potentials. *SIAM Journal on Scientific Computing*, 29(2):515–538, 2008.

[15] S. Jin, H. Liu, S. Osher, and Y.H.R. Tsai. Computing multivalued physical observables for the semiclassical limit of the Schrödinger equation. *Journal of Computational Physics*, 205(1):222–241, 2005.

[16] S. Jin, P. Qi, and Z. Zhang. An Eulerian surface hopping method for the Schrödinger equation with conical crossings. *SIAM Multiscale Modeling and Simulation*, 9:258–281, 2011.

[17] S. Jin and D. Yin. Computational high frequency waves through curved interfaces via the Liouville equation and geometric theory of diffraction. *Journal of Computational Physics*, 227(12):6106–6139, 2008.

[18] L. Landau. Zur Theorie der Energieubertragung. II. *Physics of the Soviet Union2*, pages 46–51, 1932.

[19] C. Lasser, T. Swart, and S. Teufel. Construction and validation of a rigorous surface hopping algorithm for conical crossings. *Communications in Mathematical Sciences*, 5(4):789–814, 2007.

[20] Caroline Lasser and Stefan Teufel. Propagation through conical crossings: an asymptotic semigroup. *Comm. Pure Appl. Math.*, 58(9):1188–1230, 2005.

[21] P.L. Lions and T. Paul. Sur les mesures de Wigner. *Rev. Mat. Iberoamericana*, 9(3):553–618, 1993.

[22] P.A. Markowich, N.J. Mauser, and F. Poupaud. A Wigner-function approach to (semi) classical limits: Electrons in a periodic potential. *Journal of Mathematical Physics*, 35:1066–1094, 1994.

[23] C.C. Martens and J.Y. Fang. Semiclassical-limit molecular dynamics on multiple electronic surfaces. *Journal of Chemical Physics*, 106(12):4918–4930, 1997.

[24] G. Panati, H. Spohn, and S. Teufel. Effective dynamics for Bloch electrons: Peierls substitution and beyond. *Communications in Mathematical Physics*, 242(3):547–578, 2003.

[25] G. Panati, H. Spohn, and S. Teufel. Motion of electrons in adiabatically perturbed periodic structures. *Analysis, Modeling and Simulation of Multiscale Problems*, pages 595–617, 2006.

[26] D.S. Sholl and J.C. Tully. A generalized surface hopping method.

[27] M. Sillanpää, T. Lehtinen, A. Paila, Y. Makhlin, and P.J. Hakonen. Landau–Zener interferometry in a Cooper-pair box. *Journal of Low Temperature Physics*, 146(1):253–262, 2007.

[28] G. Sundaram and Q. Niu. Wave-packet dynamics in slowly perturbed crystals: Gradient correcti ons and Berry-phase effects. *Phys. Rev. B*, pages 14915–14925, 1999.

[29] J.C. Tully. Molecular dynamics with electronic transitions. *The Journal of Chemical Physics*, 93:1061–1071, 1990.

[30] J.C. Tully and R.K. Preston. Trajectory surface hopping approach to nonadiabatic molecular collisions: the reaction of H with D. *The Journal of Chemical Physics*, 55:562–572, 1971.

[31] E. Wigner. On the quantum correction for thermodynamic equilibrium. *Physical Review*, 40(5):749–759, 1932.

[32] C. Zener. Non-adiabatic crossing of energy levels. *Proceedings of the Royal Society of London. Series A, Containing Papers of a Mathematical and Physical Character*, 137(833):696–702, 1932.